Photochemistry and Photobiology, 20**, **: *–*

Photoinactivation Sensitivity of *Staphylococcus carnosus* to Visible-light Irradiation as a Function of Wavelength

Katharina Hoenes*[1], Ulla Wenzel[1], Barbara Spellerberg[2] and Martin Hessling[1]

[1]Institute of Medical Engineering and Mechatronics, Ulm University of Applied Sciences, Ulm, Germany
[2]Institute of Medical Microbiology and Hygiene, University of Ulm, Ulm, Germany

Received 22 July 2019, accepted 16 September 2019, DOI: 10.1111/php.13168

ABSTRACT

Inactivation properties of visible light are of increasing interest due to multiple possible fields of application concerning antibacterial treatment. For violet wavelengths, the generation of reactive oxygen species by porphyrins is accepted as underlying mechanism. However, there is still little knowledge about photosensitizers at blue wavelengths. While flavins were named as possible candidates, there is still no experimental evidence. This study investigates the photoinactivation sensitivity of *Staphylococcus carnosus* to selected wavelengths between 390 and 500 nm in 10- to 25-nm intervals. Absorption and fluorescence measurements in bacterial lysates confirmed inactivation findings. By means of a mathematical calculation in MATLAB®, a fit of different photosensitizer absorption spectra to the measured action spectrum was determined to gain knowledge about the extent to which specific photosensitizers are involved. The most effective wavelength for *S. carnosus* at 415 nm could be explained by the involvement of zinc protoporphyrin IX. Between 450 and 470 nm, inactivation results indicated a broad plateau, statistically distinguishable from 440 and 480 nm. This observation points to flavins as responsible photosensitizers, which furthermore seem to be involved at violet wavelengths. A spectral scan of sensitivities might generally be an advantageous approach for examining irradiation impact.

INTRODUCTION

The ability of visible light to reduce the viability of microorganisms has been widely recognized. The main photoinactivating properties of light are observed in the region around 405 nm. Possibilities for applications without using externally added photosensitizers open a wide range of possible applications in fields like antimicrobial therapy or medical devices (1,2) as well as food industry (3,4) or drinking water implementations (5,6). It has been shown that irradiation with visible light can lead to a reduction of microorganisms which exhibit resistance toward antibiotic treatment (7–9). Since human cells are less susceptible to visible light than microorganisms (7,9), this disinfection technique can optimally be applied in certain therapeutic treatments in the medical sector. Treatment of acne (10–12) was suggested as well as treatment of *Helicobacter pylori* infections (13–15) and periodontal pathogens in the oral cavity (16,17). Apart from direct treatment of patients, Maclean et al. (18) and Murrell et al. (19) provided ideas to disinfect surfaces in hospitals with visible light to reduce surgical site infections.

One essential parameter in this context is the wavelength of the applied light. For that matter, it is irrelevant from which kind of light source the emitted irradiation originates (20,21). The supposed mechanism implies that antimicrobial activity is based on photosensitizers (10,22). These molecules absorb radiation at specific wavelengths and induce the formation of reactive oxygen species (ROS) (23,24). This theory is supported by the oxygen dependency of irradiation experiments with visible light (25–27).

According to the literature, the region around 405 nm includes the most effective wavelengths for light application (16,20,28,29). Porphyrins have been identified as responsible photosensitizers for this effect. The induction of reactive oxygen species upon irradiation of porphyrins has been verified for pure substances (24,30,31) as well as in whole cells or lysates (32–35), indicating the involvement of porphyrins in the damaging effect. Moreover, porphyrin absorption spectra are in good agreement with the spectral maximum of the disinfection process (20,28). In several visible-light-sensitive bacterial and fungal strains, porphyrins were found by fluorescence emission, high-pressure liquid chromatography (HPLC) or mass spectrometry (10,27,32,36–43). Furthermore, the cultivation in a porphyrin precursor enriched media congruously lead to an increased antimicrobial effect. The reduction of bacteria cultured in media with supplementation of aminolevulinic acid (ALA) was higher compared to normally cultivated bacteria exposed to an identical light dose (10,22).

Several different kinds of porphyrin species with slightly different absorption spectra have been described. It is assumed that not all of them are equally involved in the photoinactivation process. Different concentrations and compositions of porphyrins were found in various bacterial strains (38), and it is assumed that the sensibility of specific microorganisms to light exposure varies due to those differences (44). While different porphyrins —mainly protoporphyrin IX (PPIX), coproporphyrin III (CPIII), and uroporphyrin (UP)—have been implicated to act as photon acceptor in microbial inactivation (36,38–40,44), there is still no agreement to which extent those three molecules are involved or to which degree each one of them is contributing to the generation of reactive oxygen species. Completely different profiles of porphyrin contents were measured for different strains (38), and even for the same strain under similar culture conditions,

*Corresponding author email: katharina.hoenes@thu.de (Katharina Hoenes)

different results of porphyrin occurrence were obtained (36,43). Moreover, further porphyrins that exist in the bacterial cytoplasm in lower intracellular concentrations may be involved (38). Quantum yields are varying for different photosensitizers, which might decouple concentration and antimicrobial impact (24). Zinc protoporphyrin IX (ZnPPIX), for example, which also exists in bacteria but has hardly been studied, possesses a quantum yield for singlet oxygen generation almost twice as high as PPIX (23). Another problem is that porphyrin concentrations also vary due to diverse experimental conditions and cultivation techniques of different research groups (39,41). Likewise, the results about the sensitivity of different strains to visible-light exposure inherited a broad diversity when a collective of literature data was reviewed (29,45).

Until now, most publications investigate and compare a maximum of two different wavelengths. There are only few studies in which authors applied a larger number of different wavelengths (20,28,46,47). Several studies came to the conclusion that wavelengths longer than 430 or 440 nm, respectively, do not have any antibacterial impact at doses similar to the ones in the violet range (20,28). To date, it is known that also wavelengths above 420 nm, especially in the blue wavelength range of 450–470 nm can have an antibacterial activity (32,42,48,49), though 2–5 time less effective than in the violet region (42,45). Therefore, doses have to be increased accordingly to reach a comparable antimicrobial effect.

Bacteria of different species and strains were found to be sensitive against irradiation in the blue range, which implies that a potential chromophore absorbing in this region has to be ubiquitously existent in various bacterial species. Flavins were named as possible photosensitizers since they can demonstrably induce ROS when irradiated, especially when used as externally supplemented photosensitizers in photodynamic therapy (PDT) (50–52). Flavins are present in practically all bacterial and fungal species (53).

To investigate the antimicrobial effect of visible light of different wavelengths, we studied the range from 390 to 500 nm against *Staphylococcus carnosus* under constant experimental conditions. We applied two different irradiation doses for each wavelength to be sure that the conditions for calculating sensitivities with a linear fitted model are given. Experiments in a broad (390–500 nm) but sufficiently resolved (10–25 nm) spectral range were conducted to allow investigation of the involved photosensitizers, due to availability of comparable wavelength sensitivities. The gained action spectrum could be employed to fit various photosensitizer absorptions to the measured wavelength sensitivities of *S. carnosus* in MATLAB®. By this means, the potential involvement of different candidate combinations can be checked for plausibility. Since there are assumptions, supposing flavins as possible photosensitizer candidates in the blue wavelength region, but no experimental evidence so far, we aimed to get knowledge about the involvement of flavins at irradiation with visible light. Absorption and fluorescence measurements support the results of our irradiation experiments. Furthermore, the advantages of generally applying an action spectrum for irradiation approaches with visible light could be examined by this means.

MATERIALS AND METHODS

Microorganism. Bacteria investigated in this study were *S. carnosus* DSM20501 (DMSZ, Deutsche Sammlung von Mikroorganismen und Zellkulturen, Braunschweig, Germany). M92 medium contained 30 g tryptic soy broth (Sigma-Aldrich Chemie GmbH, München, Germany) and 3 g yeast extract (Merck KGaA, Darmstadt, Germany) for 1 L medium. The test strain was inoculated in an overnight culture of 3 mL M92 for 16 h at rotary conditions (170 rpm) at 37°C. Two hundred microliters of this preculture was transferred to 30 mL M92 at 37°C (170 rpm) for 4 h until mid-exponential phase was reached and the population density was adjusted to 5×10^7 CFU mL^{-1} (colony-forming units per milliliter) by optical density measurement. The broth was centrifuged at 7000 ***g*** for 5 min and the resultant pellet resuspended in phosphate-buffered saline (PBS). After a further washing step in PBS, the suspension was used for experimental purposes.

Visible-light sources. Different light-emitting diodes (LEDs) were used for irradiation experiments at various wavelengths between 390 and 500 nm. As manufacturer declarations often differ from the real peak emission values or fluctuate between each production batch, the emission spectrum of each LED was measured with a spectrometer (SensLine AvaSpec-2048 XL, Avantes, Apeldoorn, The Netherlands) at its operating current, after a preheating interval (Fig. 1). In Table 1, specific details of each LED as well as the respective bandwidths are indicated. Each LED was cooled actively during the experiments to avoid heating up the bacterial sample. At the wavelength region around 450 nm, where flavins are supposed to play a role as photosensitizers, intervals of 10 nm have been realized. Due to a mean LED emission bandwidth of 25 nm, it is not expedient to apply smaller intervals when working with LEDs as a light source. At lower wavelengths around 405 nm, where porphyrins have their maximum absorption, 10- to 20-nm intervals have been achieved. Therefore, the whole-spectral region between 390 and 500 nm could be covered with the following LEDs in the order of the table below giving the number and the manufacturer: LZ4-40UB00-00U4 (LED Engin, Inc., San Jose, CA, USA), LZ4-40UB00-00U8 (LED Engin, Inc.), IN-3531SCUV-U70 (Innolux Corp., Santa Clara, USA), EOLS-440-227 (Epigap Optronic GmbH, Berlin, Germany), LZ4-00B208 (LED Engin, Inc.) XPEBRY-L1-0000-00Q01 (Cree, Inc., Durham, NC, USA), XPEBBL-L1-0000-00301 (Cree Inc.), 941-XQEBLU0000305 (Cree, Inc.), NCSE219BT-V1 (Nichia corp., Anan, Japan).

Exposure experiments. For the experimental setup, 1.5 mL volume of the bacterial suspension at a density of 5×10^7 CFU mL^{-1} was transferred to a 5-mL beaker glass, resulting in a filling height of 1 cm. The intensity of the different LEDs was maintained constant at 21 mW cm^{-2} by adapting the operating current for each LED type. This specific irradiation intensity was chosen because it is the maximum value that can be reached with the weakest LED. Intensity measurements were performed with an optical power meter OPM150 with the UVS measuring head for 190–1100 nm (Qioptiq, Göttingen, Germany) at the beginning of the experiment and at each sample drawing interval. Maximal fluctuations in the light intensity have been 21.0 ± 0.6 mW cm^{-2}. The beaker glass was placed in a small deepening on a black surface to only allow the previously measured radiance to affect the sample. It was ascertained in pre-experiments that a white surface would potentiate the irradiation by reflection in an indefinite extent without being properly measurable and will have a noticeable impact on the bacterial behavior compared to an absorbing surface that only allows radiation from above. The LED was placed on top of a truncated hollow pyramid (54) with a highly reflective inside to achieve a homogenously irradiated sample area (Fig. 2). At the beginning of the experiment as well as at each sampling interval, the sample temperature was measured contactless with an infrared thermometer Raynger MX (Raytek Fluke Process Instruments GmbH, Berlin, Germany). Although the LEDs were cooled actively, the temperature in the irradiated samples was slightly higher than in control samples (difference of 4°C in average). The maximal temperature did not exceed 30°C. With optimal growth conditions being 37°C for *S. carnosus,* the possibility of unintended heat inactivation could therefore be excluded.

Bacterial enumeration and statistical analysis. Samples were drawn after homogenizing the bacterial culture and were diluted serially in PBS. Five hundred microliters of diluted samples was filtered through cellulose acetate filters with a pore size of 0.45 µm (Sartorius, Göttingen, Germany) by means of a vacuum pump. Filters with retained bacteria were placed on moistened nutrient disks for staphylococcal detection (Chapman NKS 14074--50, Sartorius AG). After incubation for 48 h at 37°C, plates were enumerated manually. The resultant counts were converted into CFU mL^{-1}. Each experiment for a certain wavelength was performed in triplicate. Significance of the light treatment was calculated for each point at the 95% confidence interval compared to the

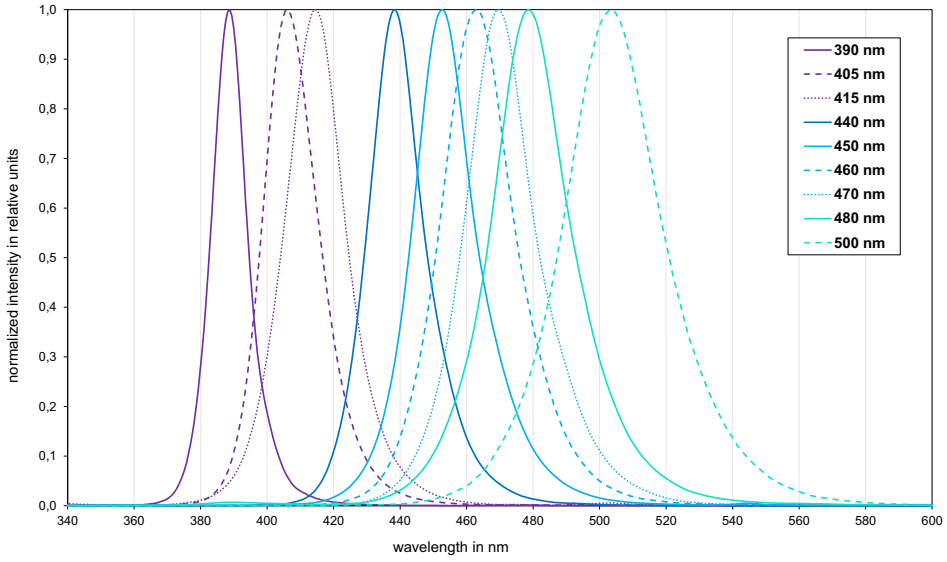

Figure 1. Normalized emission spectra of light-emitting diodes used for irradiation experiments.

Table 1. Measured peak emission wavelengths and bandwidths of employed LEDs.

Declaration (nm)	385	405	420	440	457	465	465–485	480	Blue-green
Measured peak (nm)	388.7	405.9	414.3	438.5	452.7	463.3	469.2	478.7	503.4
Bandwidth half max. (nm)	12.17	18.97	20.44	18.92	21.26	24.78	23.88	27.10	33.5

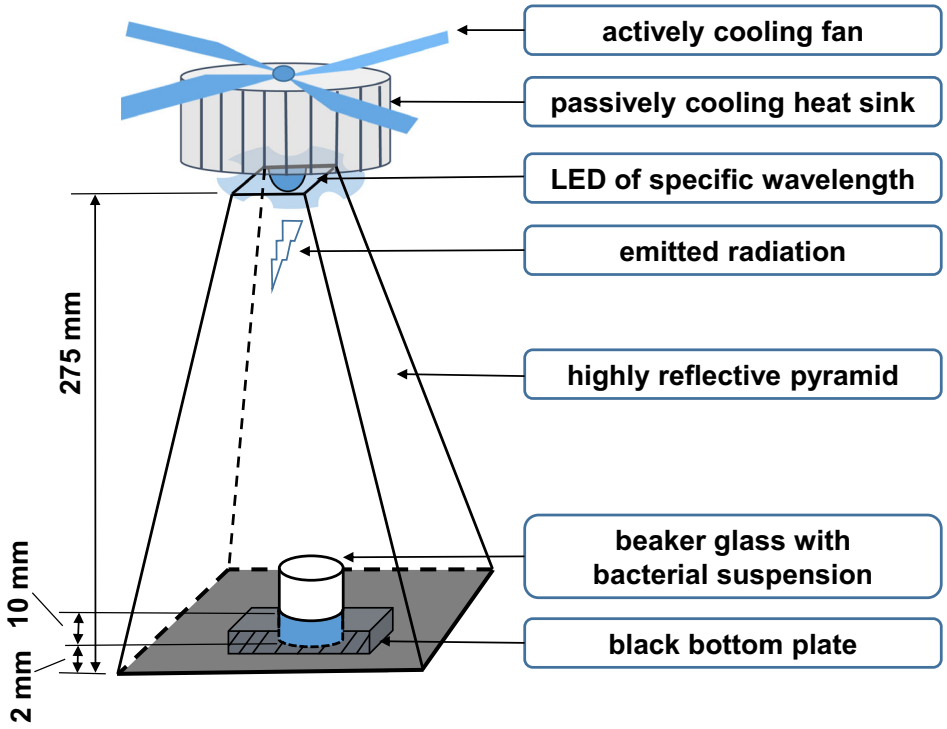

Figure 2. Schematic irradiation setup for exposure experiments with different LED wavelengths. Multiple reflection inside of the pyramid leads to homogenous irradiation in the sample area and black bottom plate ensures exclusive irradiation from above as measured with power meter.

untreated control using the dependent t-test with IBM SPSS (release 25). Calculated bacterial sensitivity ($\log_{10}$ reduction related to the applied dose) at different wavelengths was statistically compared by ANOVA (IBM SPSS, release 25).

Calculation of bacterial sensitivity at each wavelength. For comparing the impact of each wavelength on viable bacterial counts, a suitable parameter had to be calculated. In contrast to earlier studies, two doses were probed for each wavelength. For a long time, it was assumed that the relationship between applied dose and colony reduction is based on an exponential behavior resulting in a linear progression when presented logarithmically. Some studies, however, detected nonlinear shapes, especially at the beginning of the irradiation process. This phenomenon, called "shoulder" in the following, can be explained by the need to initially build up a certain ROS concentration to overcome bacterial repair mechanisms.

In this study, a linear behavior is assumed for the calculation of sensitivity to a certain irradiation wavelength. Compared to other studies, doses were not fixed but adapted appropriate to the employed wavelength (Fig. 3) to avoid the conclusion that a wavelength is less effective just because the steep part of the slope has not been reached yet with the applied dose. In fact, it was aimed to reach a certain $\log_{10}$ reduction in CFU with a fixed intensity and the duration of irradiation was varied per wavelength to gain specific dose levels. For this study, we wanted to obtain a $\log_{10}$ reduction >1 $\log_{10}$ for the first dose and between 2.5 and 3.5 $\log_{10}$ for the second dose. This minimizes the risk of falsified efficiency values based on the shoulder at the beginning of the progression, as probed values lie within the linear part of the slope. The calculated value may not match exactly for each dose when extrapolating due to mentioned nonmonoexponential shoulders but it represents the overall disinfection capacity of a wavelength and is therefore a good parameter for comparison.

The $\log_{10}$ reduction was calculated for both doses related to the starting concentration and each was divided by the applied dose, resulting in a value with the unit $cm^2\ J^{-1}$, which represents the reduction that can theoretically be achieved with a dose of 1 J cm^{-2} of this wavelength. The results for the two doses were averaged to form a single value. By means of this wavelength-comparable parameter, an action spectrum can be depicted as distribution plotted over the wavelength spectrum between 390 and 500 nm.

Calculation of proportions of involved photosensitizers. With the availability of an action spectrum of a certain strain, conducted under constant external conditions, and with the presumption of a steady photosensitizer concentration (c) over the experimental duration as well as between the single experiment performances due to equal cultivation, it is possible to estimate the contribution of putatively involved photosensitizers based on their absorption spectra. The disinfectant value (dv) is based on numerous parameters but is directly proportional to I_{abs}, the absorbed irradiation. Strictly speaking, not the absorption but the absorbed photons are relevant for the generation of ROS and at the same intensity there are more photons at longer wavelengths. This effect would probably reduce the impact of lower wavelengths a bit, but to an extent that it was considered negligible here.

For monochromatic light with the wavelength λ, it applies:

$$I_{abs}(\lambda) = I_0(\lambda)\,(1-\exp(-c\,\varepsilon(\lambda)x)) \tag{1}$$

In Lambert–Beer's law, $I_0 = I_0(\lambda)$ is the applied irradiation intensity at a certain wavelength, c the concentration of the photosensitizer addressed, $\varepsilon = \varepsilon(\lambda)$ the molar absorption coefficient of the photosensitizer and x the absorption length. For small coefficients, a first-order Taylor series approximation ($\exp(x) \approx 1 + x$) is possible, which applies here due to small photosensitizer concentrations.

$$I_{abs}(\lambda) \approx I_0(\lambda) c\,\varepsilon(\lambda) x \tag{2}$$

or

$$dv_\lambda = \text{const}\ I_0\ (\lambda)\,\varepsilon(\lambda) \tag{3}$$

As light-emitting diodes are not monochromatic, the disinfecting effect of specific LED spectra has to be calculated:

$$dv = \sum_\lambda dv_\lambda = \sum_\lambda \text{const}\, I_0(\lambda)\,\varepsilon(\lambda) = \text{const} \sum_\lambda I_0(\lambda)\,\varepsilon(\lambda) \tag{4}$$

when summed up, the product of the LED spectrum and the photosensitizer absorption is proportional to the measured disinfection effect at a specific wavelength. Since there is more than one photosensitizer (ps_1, ps_2, ... ps_i) to which hitherto considerations similarly apply, the overall disinfection value dv_{ov} for a single LED is calculated as follows:

$$dv_{ov} = \sum_i dv_i = \sum_i (\text{const}_i \sum_\lambda (I_0(\lambda)\,\varepsilon_i(\lambda))) \tag{5}$$

The constants const_i, one for each photosensitizer considered, are adjusted to values resulting in the best fit for the spectral distribution of the measured disinfection data and can give knowledge about the probable participation of this photosensitizer on the colony-reducing effect. The calculation of the specific constants was performed by a fit in

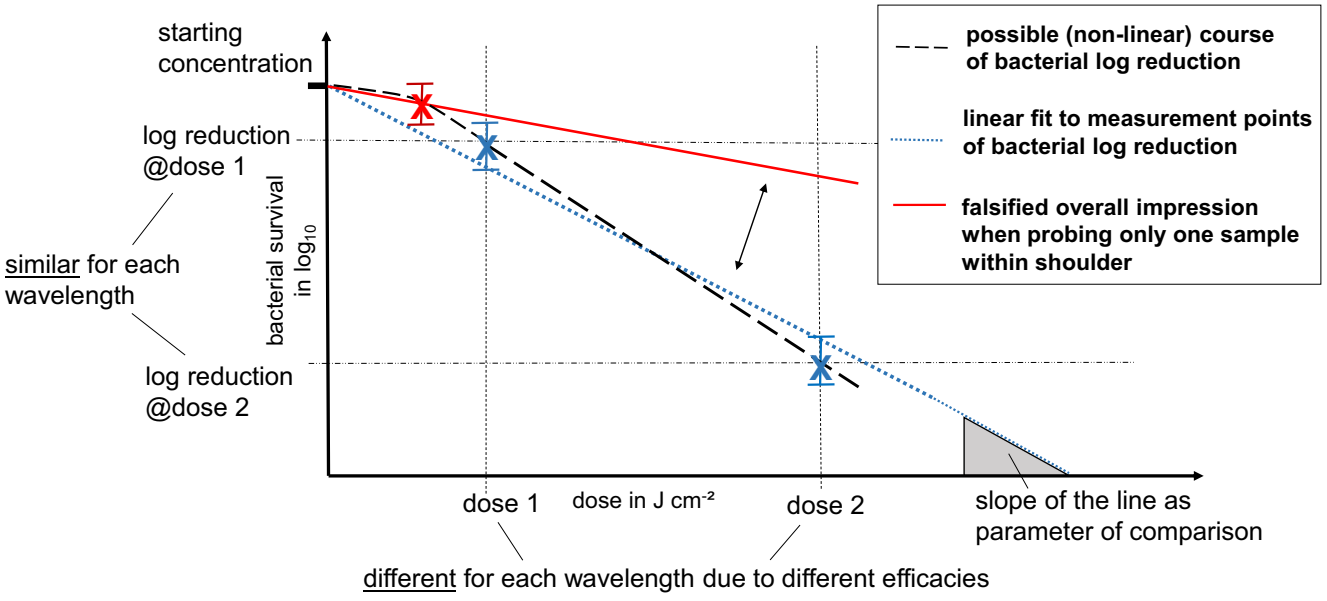

Figure 3. Schematic diagram for explaining the consideration of nonmonoexponential bacterial growth reduction at the usage of a linear model with at least two data points: probing at only one fixed dose might lead to a falsified overall reduction impression.

MATLAB® R2018a. The command "lsqcurvefit" was used to compare all available spectra and assessing their relevance.

For obtaining the necessary absorption spectra underlying this calculation, relevant photosensitizers were dissolved in PBS or dimethyl sulfoxide (DMSO) and their absorption measured in a cuvette spectrometer Specord Plus (Analytik Jena, Jena, Germany) as shown in Fig. 4. As porphyrins are hardly solvable in PBS, pH was elevated over pH 10 for better solubility and subsequently reduced to pH 7.0 again.

Absorption and fluorescence measurements on bacterial lysates. For the analysis of relevant photosensitizers, absorption and fluorescence measurements were conducted. 2 mL of a culture used for the irradiation experiments, with 5×10^7 CFU mL^{-1} at exponential phase, was washed in PBS as described before and lysed mechanically with glass beads in a cell disrupter Savant Bio101 (Thermo Fisher Scientific corp., Waltham, MA, USA). Cell debris was centrifuged subsequently to obtain a clear solution. The absorption of this cell extract was measured in a cuvette spectrometer Specord Plus (Analytik Jena). For comparison with the absorption, fluorescence excitation spectra were recorded at fluorescence emissions of the lysate with a Clariostar microplate reader (BMG Labtech, Ortenberg, Germany).

Furthermore, the fluorescence signals of the current culture and a culture incubated for 25 days at room temperature were measured using a violet 405-nm Flexpoint laser (Laser Components, Olching, Germany) for excitation coupled into a fluorescence light probe (Ocean Optics, Largo, FL, USA). Its tip was placed inside the cuvette while the fluorescence was detected by a spectrometer (SensLine AvaSpec-2048 XL, Avantes).

RESULTS

Bacterial reduction and sensitivity at each wavelength

The results of the bacterial counts at different wavelengths are presented in Table 2 and Fig. 5a,b. Calculation of $\log_{10}$ reductions is based on the measured inoculum concentration of each experiment, which has been adjusted to approximately 5×10^7 CFU mL^{-1} prior to irradiation. The logarithmic representation of the axis of ordinates leads to a straight line for exponential reductions. It can be noticed that for the first dose applied a reduction above 1 $\log_{10}$ could not always been achieved. For 17.5 J cm^{-2} at 415 nm, 35 J cm^{-2} at 440 nm and 140 J cm^{-2} at 480 nm, only 0.6610, 0.9190 and 0.6448 $\log_{10}$ reduction were determined, respectively, for the reduction of the ability to form CFU. In Fig. 5a, where wavelength results for 390–440 nm are depicted, it can be observed that the second part of the slope is even steeper than the first. This is especially notable for 415 nm irradiation and probably caused by the first measurement still lying in the range of the shoulder part of the curve. At 500 nm for both doses applied, no real inactivation effect has been noticed. Figure 5c exemplary demonstrates the

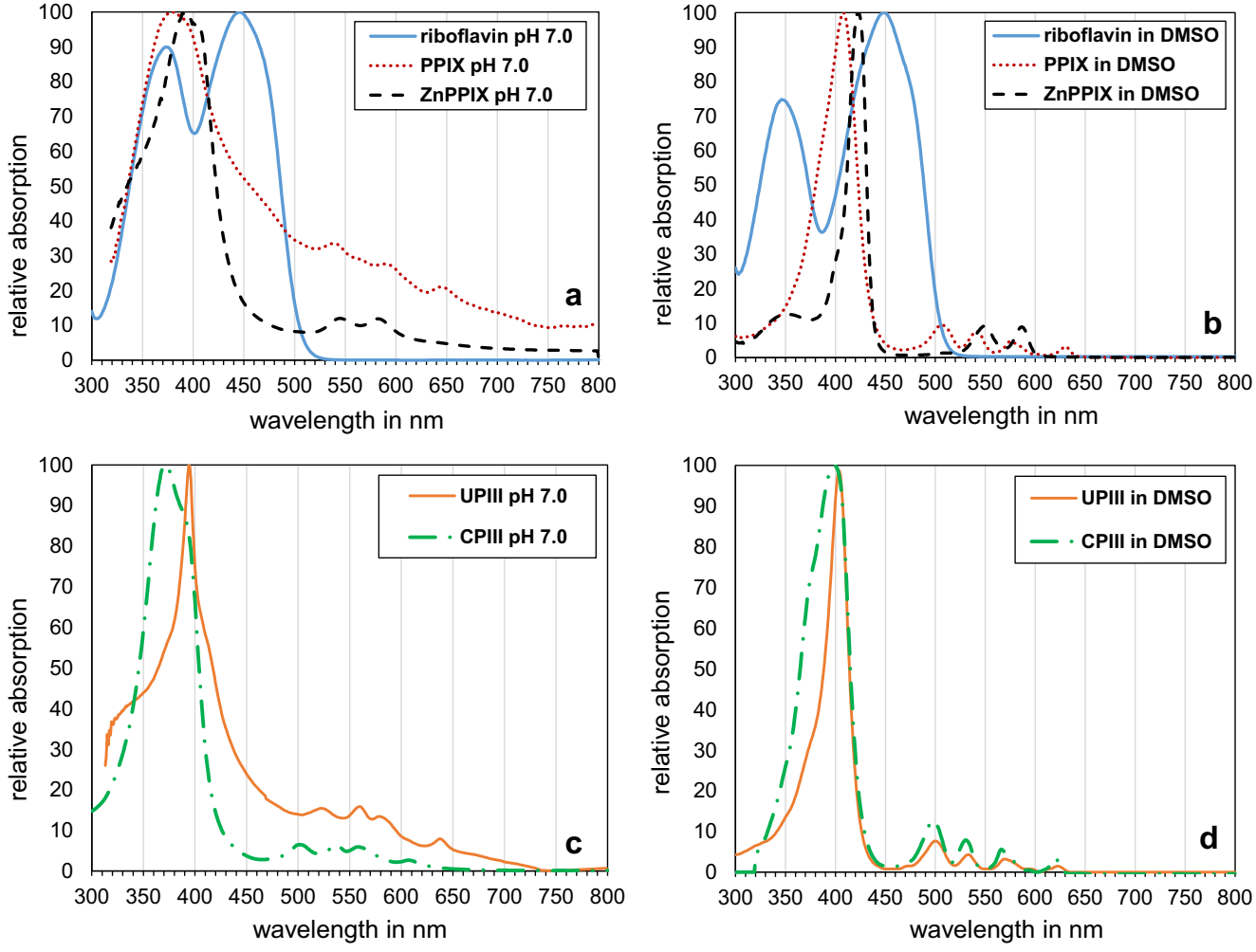

Figure 4. Normalized absorption spectra of pure photosensitizers dissolved in PBS (a, c) or DMSO (b, d).

Peak wavelength (nm)	Dose (J cm^{-2})	Time (h: min:s)	Log_{10} reduction (mean)	SD−log_{10}	Sensitivity (log_{10}/ J cm^{-2})	SD-sens.	Dose per 1 log_{10} (J cm^{-2}/ log_{10})
390	11.6	00:09:12	1.300	0.663	0.146	0.035	6.86
	17.5	00:13:50	2.711	0.438			
405	35	00:27:50	1.381	0.184	0.048	0.006	20.83
	70	00:55:30	3.558	0.157			
415	17.5	00:13:50	0.661	0.112	0.078	0.032	12.78
	35	00:27:50	3.461	0.247			
440	35	00:27:50	0.919	0.549	0.039	0.012	25.95
	70	00:55:30	3.064	0.347			
450	140	01:51:00	2.684	0.532	0.019	0.003	53.42
	210	02:46:40	3.231	0.251			
460	70	00:55:30	1.193	0.088	0.017	0.002	60.04
	140	01:51:00	2.561	0.181			
	210	02:46:40	3.215	0.288			
470	140	01:51:00	2.004	0.244	0.016	0.001	61.40
	210	02:46:40	3.208	0.337			
480	140	01:51:00	0.645	0.238	0.006	0.003	182.47
	210	02:46:40	1.471	0.271			
500	140	01:51:00	0.261	0.220	0.002	0.001	573.90
	210	02:46:40	0.292	0.073			

Table 2. Results of irradiation experiments with constant intensity of 21 mW cm^{-2}. Standard deviation (SD) of log_{10} reduction from measurements within each dose and SD of sensitivity from dose-related measurement values of all doses of one wavelength. A value giving the necessary dose for 1 log_{10} reduction is calculated as reciprocal of sensitivity.

inactivation progression of *S. carnosus* for irradiation at 460 nm. The mentioned shoulder can clearly be observed.

The differences between the values of irradiated samples and associated controls (not shown here) were found to be normally distributed, except for the 460 nm values at 140 J cm^{-2}, as assessed by the Shapiro–Wilk test ($P = 0.037$). The paired *t*-test verified a significant difference in bacterial reductions between irradiated sample and control for all values besides the samples exposed to 500 nm 140 J cm^{-2}, $t(2) = 2.057$, $P = 0.176$. Cohen's d scored values over 0.8 for all measurements (minimal value 1.19 for 500 nm 140 J cm^{-2}) indicating a strong effect.

For comparing the antimicrobial effects of different wavelengths with each other, the sensitivity was calculated as described above by relating the achieved log_{10} reduction in colony counts to the applied dose at a certain wavelength. The resultant values in cm^2 J^{-1}, which describe the log_{10} reduction theoretically achievable per J cm^{-2}, are plotted over the wavelength in Fig. 7. This so-called action spectrum can be used to assume the sensitivity of a strain to irradiation with a certain wavelength and to draw conclusion about involved photosensitizers.

For statistical comparison of the applied wavelengths, a one-way ANOVA was conducted based on the sensitivity data. Data were divided into nine categories referring to the applied wavelengths. Sensitivity data were found to be normally distributed within the wavelength groups as assessed by the Shapiro–Wilk test ($\alpha = 0.05$), with the lowest value of $P = 0.068$ at 440 nm. Homogeneity of variances was asserted using Levene's test, which demonstrated that equal variances could not be assumed ($P < 0.001$). Therefore, Welch's ANOVA and the Games–Howell post hoc analysis were considered in the following. The sensitivity differed statistically significant for different wavelengths, Welch's $F(8,53) = 15.781$, $P < 0.001$.

Games–Howell *post hoc* analysis (Fig. 6) revealed a significant difference between 500 nm and all other groups besides the 480 nm group and vice versa. There is also no significant difference between 440, 450, 460 and 470 nm. Additionally, the 440 nm group shows no significant difference compared to 415 and 405 nm and therefore is only significantly different compared to 390, 480 and 500 nm. There was furthermore no significant difference between 405 and 415 nm.

As the main interest here was to detect a possible peak at the wavelengths around 450 nm to clarify flavins as involved photosensitizers, combined contrasts were additionally calculated as follows: 450, 460 and 470 nm were compared with each other, respectively, in a single contrast. Since no significant differences were observed, they were grouped and compared with 440 and 480 nm, respectively, to outline the borders of the "peak." 450 nm (M = 0.0187, SD = 0.0032), 460 nm (M = 0.0167, SD = 0.0020) and 470 nm (M = 0.0163, SD = 0.0014) were significantly lower than the sensitivity at 440 nm (M = 0.0385, SD = 0.0119) with a mean difference of 0.0213 (SE = 0.0070), $P = 0.003$ and significantly higher than 480 nm data (M = 0.0055, SD = 0.0025) with a mean difference of 0.0117 (SE = 0.0066), $P = 0.080$.

Calculated photosensitizer involvement

Based on the knowledge of the spectrally dissolved strain sensitivity to visible light, the theoretical involvement of certain photosensitizers was examined according to their absorption spectra. The continuous line in Fig. 7 represents the fit that was calculated by the function "fit" in MATLAB® R2018a referring to the absorption spectra of ZnPPIX and riboflavin shown in Fig. 4 and based on the bacterial measurements demonstrated as sensitivities.

Previously another fit was executed with "lsqcurvefit" using "trust-region-reflective" algorithm, incorporating spectra of riboflavin and the porphyrins uroporphyrin III, coproporphyrin III, protoporphyrin IX, and zinc protoporphyrin IX dissolved in PBS at pH 7.0 or DMSO. The measurement value for 390 nm was discarded from the action spectrum for the fit as the log_{10} reduction is extremely high and may result from other effects or photosensitizers not considered here. Different solvent media were used to account for explicitly differing spectra (Fig. 4). As the absorption of different flavin species are quite similar, riboflavin stands exemplary for all of them.

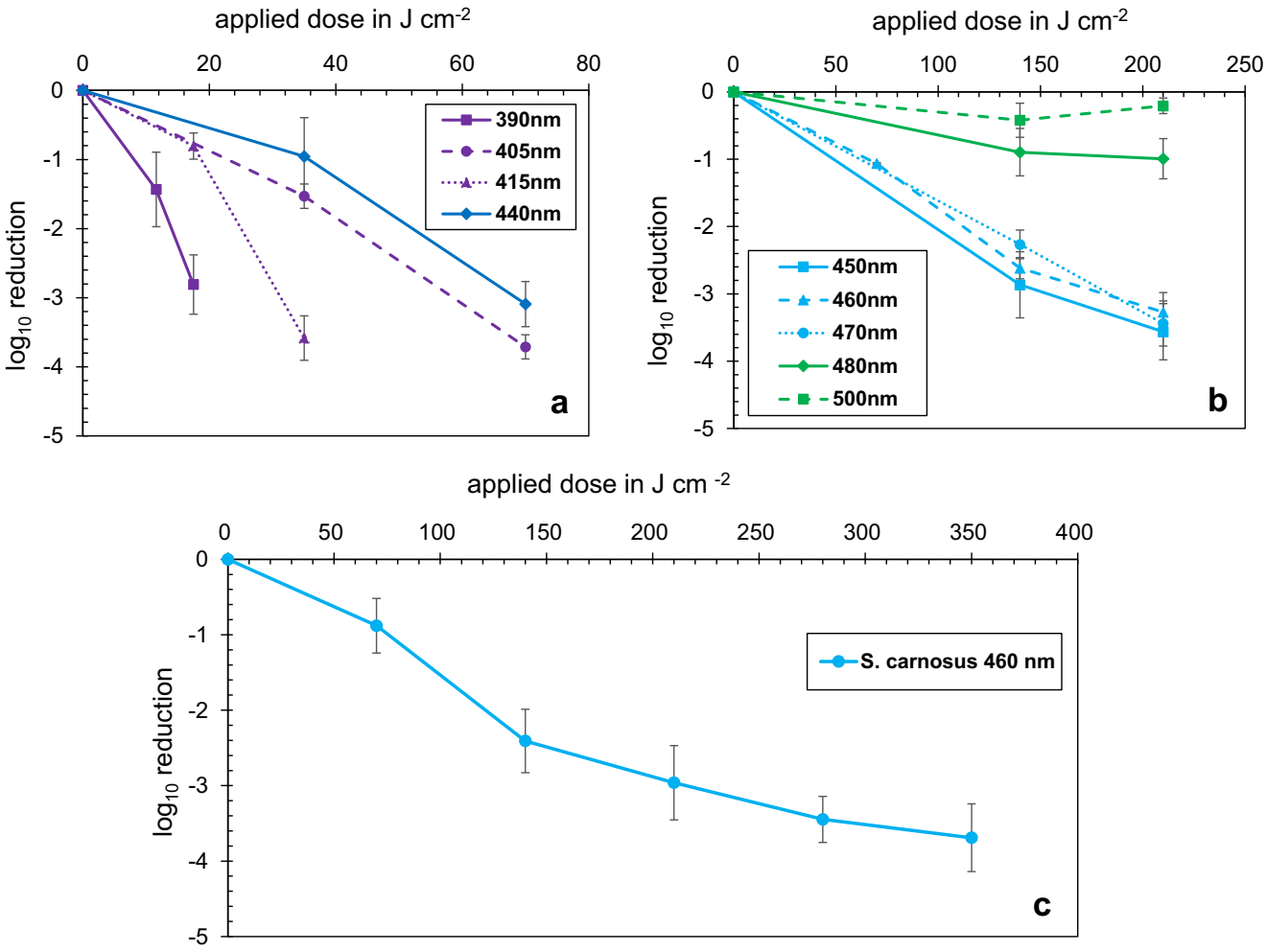

Figure 5. Bacterial reduction based on CFU counts for irradiation wavelengths from 390 to 440 nm (a) and 450 to 500 nm (b). Mean values of at least three independent experiments are plotted over the applied dose with error bars indicating the standard deviation. Exemplary inactivation progression of *S. carnosus* at 460 nm irradiation (c). Mean values of at least four independent measurements for 70–210 J cm^{-2} and two independent measurements for 280 and 350 J cm^{-2} with error bars indicating the standard deviation.

wavelength in nm	390	405	415	440	450	460	470	480	500
390		0.030	0.115	0.017	0.012	0.011	0.011	0.008	0.007
405	0.030		0.367	0.682	0.000	0.000	0.000	0.000	0.000
415	0.115	0.367		0.175	0.030	0.026	0.025	0.011	0.009
440	0.017	0.682	0.175		0.089	0.062	0.059	0.010	0.007
450	0.012	0.000	0.030	0.089		0.816	0.627	0.000	0.000
460	0.011	0.000	0.026	0.062	0.816		1.000	0.000	0.000
470	0.011	0.000	0.025	0.059	0.627	1.000		0.000	0.000
480	0.008	0.000	0.011	0.010	0.000	0.000	0.000		0.089
500	0.007	0.000	0.009	0.007	0.000	0.000	0.000	0.089	

Figure 6. Calculated significances from Games–Howell post hoc test comparing all applied wavelengths with each other. Red colored boxes in different shades indicate nonsignificant values ($\alpha = 0.05$), while green boxes show where wavelengths lead to significantly different inactivation results.

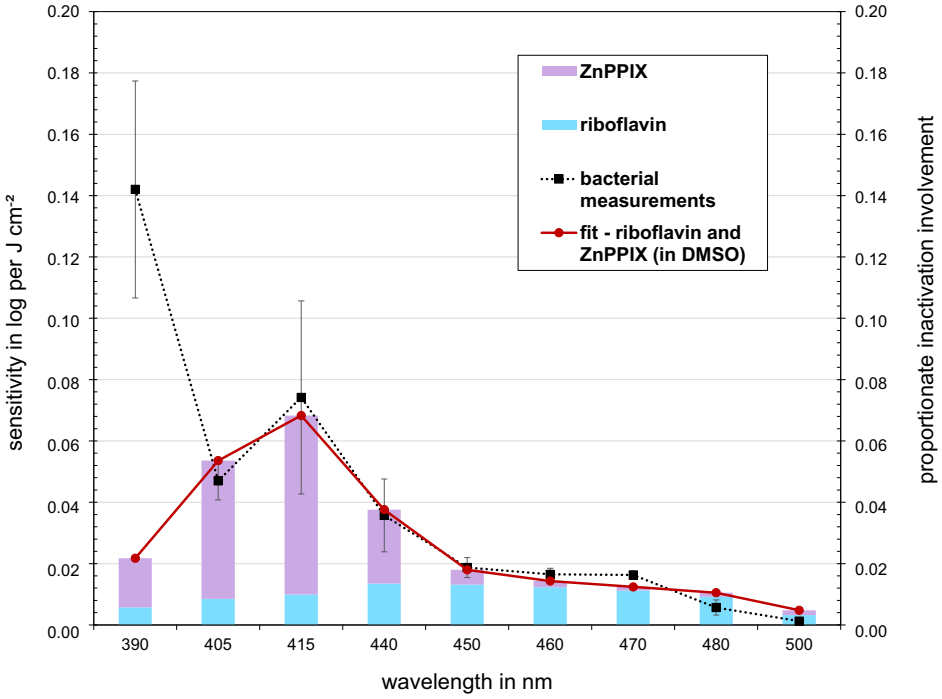

Figure 7. Action spectrum for *S. carnosus* in the wavelength range between 390 and 500 nm for the applied LEDs is illustrated by the dotted line. Data points illustrate the average of calculated sensitivities for both applied doses per wavelength with error bars indicating the standard deviation of all single values in $\log_{10}$ per J cm^{-2}. On the axis of abscissas, wavelengths are plotted unevenly distributed. The continuous line demonstrates the calculated fit of absorption spectra for ZnPPIX and riboflavin with their proportionate involvement as columns.

Since there were only 8 LED wavelengths with bacterial measurements on which the fit could be based, not all 10 measured single substance spectra could be fitted simultaneously because of restrictions of the algorithm applied. Consequently, one fit was calculated with all 5 spectra dissolved in PBS at pH 7.0 and another with the other 5 spectra with the photosensitizers dissolved in DMSO. For each photosensitizer, respectively, the fit was resulting in a coefficient, indicating the portion to which extent each spectrum contributes to the measured antimicrobial effect. Analyzing the results, it could clearly be observed that the main contributors to the disinfection seem to be riboflavin and ZnPPIX. Respectively, the coefficients calculated for these two photosensitizers were more than 2 orders of magnitude higher than the ones for the other substances. Another execution of "lsqcurvefit" with the four spectra of ZnPPIX and riboflavin, each dissolved in either PBS pH 7 or DMSO, resulted in riboflavin and ZnPPIX, both dissolved in DMSO, to be the best candidate substances to explain the action spectrum.

Subsequently performed calculation with "fit" (only two spectra allowed) achieved an R^2 of 0.9684 at a confidence interval of 95 % with riboflavin in DMSO at 0.0135 (0.007064, 0.01993) and ZnPPIX in DMSO at 0.05837 (0.04766, 0.06908). The calculated proportions of the fit according to disinfection values assigned to each photosensitizer are presented in Table 3. The percentage values are indicating to which extent the specific photosensitizer is most likely responsible for the antimicrobial effect.

The calculated fit from the spectra of ZnPPIX and riboflavin in DMSO (Fig. 7) is in good agreement with the measured antimicrobial effect of the applied wavelengths of LED irradiation. Only for 470 nm, there is a slightly higher reduction result in bacterial measurements observed than predicted by the fit. In addition, the antimicrobial effect decreases steeper to 480 nm in the bacterial measurements than the fit. With ZnPPIX and riboflavin in DMSO as contributing candidates, the fit predicts a clearly lower value than reached experimentally.

Absorption and fluorescence measurements

The absorption, measured in a bacterial lysate prepared from the same culture conditions as used in the irradiation experiments, is depicted in Fig. 8a. On a steadily decreasing background absorption to longer wavelengths, a wide peak was observed in the range between 395 and 435 nm. By fitting a Bessel spline to the decreasing curve, the bump could be carved out as distinct peak

Table 3. Results of the "fit" calculated in MATLAB® R2018a with sensitivity values from Table 2 and absorption spectra of ZnPPIX and riboflavin in DMSO shown in Fig. 4.

LED peak (nm)	FitZnPPIX and riboflavin in DMSO	Riboflavin (DMSO)	ZnPPIX (DMSO)	Riboflavin [%]	ZnPPIX [%]
390	0.0217	0.0057	0.0160	26.4	73.6
405	0.0536	0.0085	0.0451	15.9	84.2
415	0.0683	0.0099	0.0584	14.5	85.5
440	0.0376	0.0135	0.0241	35.9	64.1
450	0.0180	0.0132	0.0048	73.2	26.8
460	0.0143	0.0123	0.0020	85.8	14.2
470	0.0124	0.0112	0.0012	90.2	9.8
480	0.0105	0.0092	0.0013	87.2	12.8
500	0.0048	0.0032	0.0016	67.3	32.7

with a maximum at 422 nm. By comparing it with the absorption peaks of several known bacterial photosensitizers, we found that this peak is compatible with a mixture of protoporphyrin IX and a larger amount of zinc protoporphyrin IX.

The fluorescence measurements (Fig. 8b) were conducted in the same samples used for the absorption measurements and additionally in a culture cultivated for 25 days at room temperature. For laser excitation at 405 nm, no detectable fluorescence could be observed in the range between 540 and 600 nm in the exponential 4 hours culture. In contrast, a huge elevation was observed in the 25 days culture with a smaller peak at 547 nm and an explicit peak at 579 nm. The second peak can be assigned to ZnPPIX, whose fluorescence fits well to the observed peak emission. The absorption maximum of this photosensitizer lies at approximately 423 nm (Fig. 8a), 18 nm higher than the excitation wavelength of 405 nm, but nevertheless, the bacterial content of ZnPPIX in the 25 days culture seems to be high enough to generate an explicit fluorescence signal. For the 547 nm peak, flavin is a possible candidate. Even if its absorption maximum lies at approximately 450 nm, there still seems to be sufficient absorption at the excitation wavelength of 405 nm to achieve a fluorescence signal (Figs. 4 and 8b).

For fluorescence emission of the 25-day culture, furthermore a peak is detectable at 628 nm while for the 4-hour culture peaks can be observed at 619 and 682 nm. Those peaks are compatible with porphyrin fluorescence. The peak at 619 nm in the 4-hour culture matches the emission of CPIII (maximum at 621 nm, not shown), while the peak at 628 nm in the 25-day culture could be assigned to either PPIX (maximum at 631 nm, not shown) or to a mixture of CPIII and ZnPPIX (second peak at 639 nm, not shown). A mixture of CPIII and ZnPPIX seems to be the more likely hypothesis due to the detection of CPIII in the 4-h culture (measured fluorescence peak at 619 nm) and the main peak of ZnPPIX (measured fluorescence peak at 579 nm) in the 25-day culture.

An excitation scan of the lysate prepared from a 4-hour culture was conducted for an emission wavelength of 586 nm, where the fluorescence maximum of ZnPPIX is situated. After eliminating the riboflavin excitation, a relatively broad peak arises with its maximum at 414 nm (Fig. 8c).

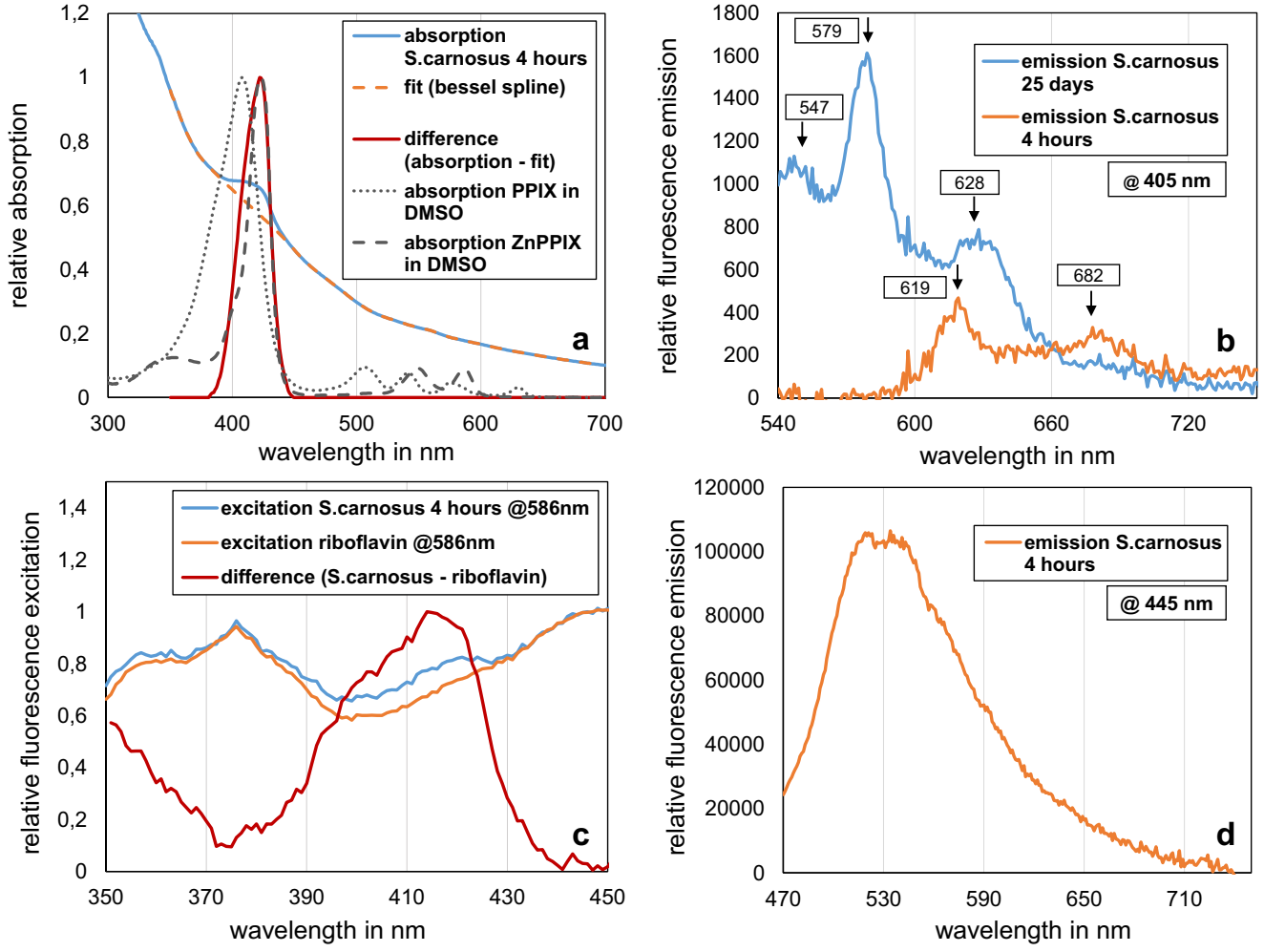

Figure 8. Absorption of *S. carnosus* lysate of an exponential culture like in irradiation experiments, fitted with a Bessel spline for background elimination and resulting absorption peak. Additionally, PPIX and ZnPPIX absorption in DMSO is shown (a). Fluorescence emission of *S. carnosus* exponential culture (4 h) and after 25 days of incubation with laser excitation at 405 nm. Spectra are recorded with different integration times (b). Excitation spectra of exponential *S. carnosus* culture (4 h) and riboflavin at 586-nm emission wavelength and resulting peak of the difference (c). Fluorescence emission of *S. carnosus* exponential culture (4 h) with excitation in a microplate reader at 445 nm (d).

Fluorescence emission was also measured in a 4-hour culture at an excitation wavelength of 445 nm in a microplate reader (Fig. 8d). The resulting spectra can be assigned to flavin fluorescence.

DISCUSSION

Earlier studies with multiple wavelengths and common pitfalls

The irradiation experiments at different wavelengths demonstrate the varying susceptibility of the examined staphylococcal strain. All probed wavelengths achieve a significant antimicrobial effect, except 500 nm, where the $\log_{10}$ reduction values are not significantly differing from the nonirradiated control.

An earlier study with spectrally dissolved disinfection behavior (28) was conducted with *S. aureus* in the range between 400 and 430 nm in which a clear peak at 405 nm was identified and disinfectant properties at wavelengths above 430 nm could not be observed. With porphyrins having their absorption maximum at these wavelengths, the investigation of Maclean et al. is regarded as crucial for elucidating the mechanism behind violet light irradiation. With the same motivation, the present study was aimed to gain knowledge about the photosensitizer(s) active around 450 nm in *S. carnosus*.

Another publication studied the effect of visible light in the range between 400 and 450 nm on *Listeria monocytogenes* (20). The highest disinfection success was achieved at 405 nm with a $\log_{10}$ reduction of 1.45. In addition, a 0.04 $\log_{10}$ reduction of bacterial growth was observed at 450 nm, which was not significant compared to the nonexposed control at a 95 % confidence interval with an applied dose of 123.3 J cm^{-2}. However, a fixed dose of 123.3 J cm^{-2} for all applied wavelengths was used in this study. When taking into account that the disinfection progress with series of ascending doses is described as nonmonoexponential, an applied dose leading to a reduction of 1.45 $\log_{10}$ at 405 nm will probably not achieve a 1 $\log_{10}$ reduction with the less impactful 450 nm. The antimicrobial effect will most likely lie within the shoulder of the curve or may even only cause tolerable damage that can be repaired by the bacterial cell. As illustrated in Fig. 3, this may lead to a falsified impression of the antibacterial capacity. In the last years, several studies demonstrated a considerable bacterial reduction with an irradiance in the wavelength range around 450 nm (16,29,32,42,45,48,49) although this wavelength exerts a twofold to fivefold lower impact than 405 nm exposure.

Therefore, in this study we did not use a fixed irradiation dose but rather tried to achieve approximately the same $\log_{10}$ reduction levels for each wavelength and compared the necessary doses to achieve this disinfection goal, rather than the $\log_{10}$ reduction itself. This was a bit more time-consuming but ensured that it is possible to assume a linear model without falsifying the overall impact by shoulder effects too much. Moreover, the range of the spectral examination was extended to 390–500 nm in order to be able to detect the disinfection efficacy around 450 nm and still obtain results for the region around 405 nm as a control. We could then compare the impact of wavelength groups and their underlying photosensitizers.

Generally, the effect of growth reduction is increasing with the applied dose. Several studies suggested that the increase is solely dependent on the light dose, which is the product of time and irradiation intensity, independent of the proportion of the two parameters, at least within certain intensity limits (20). The question of the curve progression is yet not clarified. Many authors refer to a linear behavior while more recently authors noticed other progressions, with more gently descending parts, especially at the beginning. In the present study (at least), two different doses were applied for all wavelengths to map the overall disinfection progress instead of a single point of time, by building a linear fit averaging a possible nonmonoexponential shape (see Fig. 3).

Dividing the measured $\log_{10}$ reduction by the applied dose allowed to aggregate the two-dose levels per wavelength and gave the theoretically achieved $\log_{10}$ reduction per applied J cm^{-2} as sensitivity. This approach had the advantage of minimizing the risk to rely on values located in the range of the previously mentioned shoulder. As reduction levels of 2.5–3.5 $\log_{10}$ were aimed for at the second dose, additionally to reach a value over 1 $\log_{10}$ at the first applied dose, a general consideration of the antimicrobial capacity is achieved. The reciprocal of our sensitivity value gives the dose required for reaching one $\log_{10}$ level reduction.

Already years before, but sparsely cited in the current literature, action spectra have been measured to investigate the wavelength sensitivity to visible light of certain strains (46,47) considering the $1/F_{37}$ value, which represents the reciprocal of the fluence resulting in 37 % survival. However, it has to be honored that they did not only recognize a shoulder at 330–340 nm in the UV range and 390–410 nm as location of disinfectant efficacy in the violet range for the examined *E. coli* strains, but also at blue wavelengths of 460 nm up to 510 nm for *E. coli* (47).

Measured action spectrum in detail

Regarding the results from the action spectrum itself, the extremely high sensitivity value at 390 nm compared to all other wavelengths is notable at once (Table 2). On the one hand, coproporphyrin III, one of the most frequently named photosensitizers, has its absorption maximum at comparably lower wavelengths and is absorbing at 390 nm to a great extent. Not only porphyrins have their absorption maxima here or at slightly lower wavelengths. Some vitamins, like vitamin A and K-1, that have been recognized as potential photosensitizers, as well as flavin species, absorb here (55). Moreover, 390 nm is the wavelength, of those examined, nearest to the UV range. As Kjeldstad (56) detected, there are different mechanisms for near-ultraviolet and visible light, highlighted by the reaction to azide, D_2O and superoxide dismutase (SOD) combined with irradiation experiments. 390 nm lies more or less exactly between their examined wavelengths of 360 and 415 nm with 30 and 25 nm distance, respectively. It is not unlikely that already here mechanisms of UV reduction are taking place, at least in parts. As the employed 390 nm LED emits noticeable short-wavelength fractions as far as 370 nm, both UV influence and involvement of further undefined photosensitizers seem to be likely. For these reasons, the sensitivity value at 390 nm was not included in the calculation of photosensitizer involvement.

For visible-light inactivation, we reached a value of 12.78 J cm^{-2} for one $\log_{10}$ reduction for the most distinct disinfection impact between 400 and 500 nm, which we found at 415 nm. For *S. aureus,* Maclean et al. (28) reached 2.4 $\log_{10}$ at 23.5 J cm^{-2}, which is a value of 9.8 J cm^{-2} needed for a $\log_{10}$

reduction, for their prominent wavelength of 405 nm, which lies within similar magnitudes.

Our main peak of sensitivity in the violet range, however, lies at 415 nm instead of 405 nm, with the latter being mostly referred to as the most effective wavelength for visible-light irradiation in the literature. These results are supported by a study from Kjeldstad and Johnsson (46) who have also identified 415 nm as most effective when scanning the range between 320 and 440 nm for *P. acnes*, albeit the difference to 405 nm is not explicit and presumably without significance.

Interpretation of absorption and fluorescence measurements

In our view, the reason for this unexpected outcome is the photosensitizer composition of the investigated *S. carnosus* strain, which is supported by absorption and fluorescence measurements. The absorption of an equivalent culture as used in the irradiation experiments contains a broad peak between 400 and 440 nm after eliminating the background. The main peak can be found at 423 nm (Fig. 8a), which differs by approximately 20 nm from the absorption that would have been expected for PPIX absorption alone, from which the main sensitivity of bacterial strains at 405 nm is usually derived. From the distinct width of the lysate absorption peak, it can be assumed that it contains a mix from both protoporphyrin IX and zinc protoporphyrin IX, with a great extent of the latter.

Having a look at the fluorescence measurements at 405 nm excitation (Fig. 8b), a peak at 586 nm is visible additional to the peaks of the often named porphyrins uroporphyrin, coproporphyrin III and protoporphyrin IX. This peak, which has already been noticed but not identified in other bacterial species (33,57,58), points to ZnPPIX. In a culture incubated 25 days at room temperature, it represents the main peak of the spectrum, while in a culture alike the irradiated ones, incubated for 4 h, no fluorescence is visible at 586 nm. However, this peak is located in the wavelength range of the strong, descending flavin fluorescence emission and is therefore technically difficult to detect. A fluorescence excitation measurement performed in a microplate reader on a homogenized sample of the exponential culture supports the presence of ZnPPIX at a time point used for irradiation experiments. The excitation wavelength scan measured for an emission at 586 nm comes to a clear peak at 414 nm, after eliminating the flavin background (Fig. 8c). Compared to the absorption measurement of 423 nm with the spectrometer, the excitation peak measured in the microplate reader is shifted by 9 nm. Performing the same measurements with PPIX in DMSO (emission wavelength 620 nm for the excitation scan), a comparable shift of 7 nm between the maxima of the absorption measurement (408 nm) and the excitation scan (401 nm) occurs. When measuring excitation, multiple other chromophores might show additional fluorescence at the examined emission wavelength, which results in relatively broad peaks and may also result in a shift. The obviously general differences between the two measurement methods of absorption and excitation of 7–9 nm point toward a good match between the two ZnPPIX maxima and therefore the existence of this photosensitizer in an exponential 4 h culture, even though not visible in fluorescence emission measurements.

Staphylococcus carnosus is generally capable to produce ZnPPIX (59). The strain is often used in the food industry for the fabrication of meat products (60,61), making use of that same molecule for coloring of sausage products. The accumulation of high concentration of ZnPPIX occurs after a couple of days (62), which matches our observations.

Until now, metalloporphyrins have not been paid much attention concerning the antimicrobial effect of visible light. Plavskii et al. (42) even explicitly state that metalloporphyrins do not play a role in their inactivation studies as no such fluorescence was detected in their samples. The same was the case for fluorescence emission in our experiments (Fig. 8b) as it is difficult to detect ZnPPIX emission on top of the descending slope of flavin emission, but still the presence of ZnPPIX in *S. carnosus* could be verified by careful analysis of absorption and excitation spectra. Possibly not all staphylococcal strains contain metalloporphyrins at relevant levels but in our case the shift of the sensitivity peak compared to other staphylococcal studies supports this interpretation.

At the second part of the action spectrum, in the blue wavelength range, a plateau appears with no significant differences between the wavelengths 450, 460 and 470 nm. This finding is compatible with the absorption of flavins. The relatively wide fluorescence of flavin species between 470 and 650 nm was already detected in the fluorescence sample. Statistically, it is possible to define the limits of the plateau as the irradiation sensitivity significantly differs from both 440 and 480 nm inactivation, referring to calculated contrasts. Generally, the statistical analysis illustrates two separable peaks around 415 nm and from 450 to 470 nm (Fig. 6). A similar plateau in the blue region was detected in 1976 (47) at 460–510 nm when performing measurements between 320 and 550 nm with *E. coli.* A more recent review about visible-light inactivation on oral bacteria likewise observed the accumulation of data points in the region around 405 nm and 450–470 nm, when considering investigations in which more than 3 $\log_{10}$ could have been achieved (16).

Involvement of Flavin species and ZnPPIX

The hypothesis of flavins being the responsible photosensitizer for disinfection at blue wavelengths has to be substantiated by further studies. Until now, fluorescence emissions in bacterial lysates have been detected with excitation around 450 nm (32,42,63), which first of all proves the existence of a chromophore with correspondent absorption and emission spectra. At the same, time flavins are generally able to generate ROS (50–52). Cieplik et al. (32) as well as Plavskii et al. (42) could achieve a considerable reduction at 460 and 445 nm irradiation for each treated microorganism, respectively, which can lead to the conclusion that the existent flavins are the responsible photosensitizer here. Their actual involvement at the process of inactivation is, however, hard to determine since only single wavelengths have been investigated so far. Other, hitherto unknown, chromophores absorbing in the blue range might as well contribute.

Based on the observed action spectrum of several investigated wavelengths, we tried to calculate an estimation of potential photosensitizers based on their absorption spectra. As can be seen in Fig. 7, the peak in the violet range is dominated by a porphyrin, in our case probably ZnPPIX, which has a decreasing slope to longer wavelengths with still a quite remarkable share at 440 nm and a strong decrease toward 450 nm. The only sparsely lower impact of 440 nm compared to 405 nm can be explained by the assumption that ZnPPIX is involved to a great amount.

Riboflavin, used as a representative for all flavin species, as their absorption spectra do not vary widely, shows constant involvement with a slightly elaborate peak at 450 nm and a decrease from 480 nm to longer wavelengths. As correlations between porphyrin content and disinfection success are not always given, Plavskii et al. (42) postulate the presence of another bacterial photosensitizer besides porphyrins in the violet range. The involvement of flavins in the bacterial inactivation at violet light inactivation seems to be possible according to our data. The exact percentage values of different photosensitizers may vary, but porphyrin stimulation alone cannot explain the antimicrobial effects. Including flavins provides a good base for the calculation.

Furthermore, there have been inactivation studies at 405 nm on *Enterococcus faecalis* (5,8,64) and *Streptococcus pyogenes* (8) which required a dose of 96, 43.8 and 130 J cm^{-2} for *E. faecalis* and 10.8 J cm^{-2} for *S. pyogenes,* respectively, to reach a reduction of 1 $\log_{10}$ (45). However, Enterococci (65,66) and Streptococci (66) are not capable of synthesizing porphyrins. A photoinactivation mechanism solely based on porphyrins is therefore not possible. Other photosensitizers have to be active at violet wavelengths as well, to explain this phenomenon. Cieplik et al. (32) found evidence of flavin fluorescence with 350, 400 and 460 nm excitation illustrating that also in the violet wavelengths range flavins are excitable and may be involved. In conclusion, practically all bacterial strains should be sensible to violet and blue light irradiation as flavins occur ubiquitously.

Benefits and challenges of action spectra

It stands out that absorption spectra measured in DMSO delivered better results for the fit than the ones in PBS. Since bacterial cytoplasma equals rather aqueous conditions, this might be a hint to a protein-bound appearance of the photosensitizers. As absorption spectra of photosensitizers largely vary due to environmental conditions such as pH and solvent media (37,67), further research should be carried out on absorption conditions within bacteria.

It has to be considered, that even if the shape of the action spectrum seems to represent a continuous gradient dependent on the wavelength, it contains selective measurements at certain wavelengths that are a mix of the referred wavelength as well as neighboring wavelengths, as LED emissions are defined by a bell-shaped distribution (Fig. 1). The resolution of the resulting action spectrum is therefore not only based on the number of wavelengths examined but limited by the bandwidth of the LEDs used. Bandwidths of LEDs and absorption spectra of photosensitizers, respectively, lead to the fact that generating sharp peaks is technologically not possible. More likely a rather blurred representation of the active photosensitizers contained in the investigated bacterium is achievable.

Nevertheless, a spectral distribution efficacy seems generally to be a good possibility for comparing the reactions of different bacterial species to the exposure of visible light. Rather than using only selected wavelengths, an action spectrum with a spectral distribution offers the possibility to draw conclusions about the photochemical potent photosensitizers present in the examined species and the proportion of their involvement in photoinactivation. Direct comparisons between wavelengths within the experiment are possible as the equivalence of external experimental aspects is given, which often leads to problems when comparing results of different research groups. Likewise, the comparison of broad but resolved spectral behaviors would increase the comparability between measurements of different research groups. Therefore, examination of further strains with this method is recommended.

CONCLUSION

The spectral distribution of disinfection success in the blue wavelengths range represents a good match to the absorption spectrum of flavins. Flavins could therefore be involved in a photosensitizing process, even though it is not proven whether they are the only active chromophores. Until now, only the existence of flavins in the bacterial cells and their general ability to generate ROS were demonstrated, while this study presents evidence of flavins being actively involved in the antimicrobial effects of visible light. This applies not only to blue wavelengths, since the calculation of the involvement of certain photosensitizers illustrates that flavins may also play an important role at violet wavelengths. A spectral scan of sensitivities via an action spectrum might generally be advantageous for quantifying the impact of irradiation experiments, since better comparability between research groups is given through this approach and more details about chromophores can be determined. In case of the investigated strain *S. carnosus,* we detected zinc protoporphyrin IX as a relevant photosensitizer by this means, which has not been taken into account for a contribution to photoinactivation processes before.

In conclusion, with this study we provided experimental evidence of the involvement of flavin species concerning visible-light inactivation at blue wavelengths and furthermore detected the contribution of the metalloporphyrin ZnPPIX at violet wavelengths in *S.carnosus* by application of an action spectrum.

ACKNOWLEDGEMENTS—Support by the Bundesministerium für Bildung und Forschung (grant 13N15140) is gratefully acknowledged.

REFERENCES

1. Ahmed, I., Y. Fang, M. Lu, Q. Yan, A. El-Hussein, M. R. Hamblin and T. Dai (2018) Recent patents on light-based anti-infective approaches. *Recent Pat. Anti-Infect. Drug Discov.* **13**, 70–88.
2. Dai, T., A. Gupta, C. K. Murray, M. S. Vrahas, G. P. Tegos and M. R. Hamblin (2012) Blue light for infectious diseases: *Propionibacterium acnes*, *Helicobacter pylori*, and beyond? *Drug Resist. Updat.* **15**, 223–236.
3. Kim, M.-J., W. S. Bang and H.-G. Yuk (2017) 405 ± 5 nm light emitting diode illumination causes photodynamic inactivation of Salmonella spp. on fresh-cut papaya without deterioration. *Food Microbiol.* **62**, 124–132.
4. Towery, P., J. S. Guffey, S. Motts, K. Brown, G. Harrell, T. Hobson and C. Patton (2018) Sensory evaluation of cucumbers treated with blue light. *J. Allied Health* **47**, e17–e21.
5. Lui, G. Y., D. Roser, R. Corkish, N. J. Ashbolt and R. Stuetz (2016) Point-of-use water disinfection using ultraviolet and visible light-emitting diodes. *Sci. Total Environ.* **553**, 626–635.
6. Schmid, J., K. Hoenes, M. Rath, P. Vatter, B. Spellerberg and M. Hessling (2017) Photoinactivation of *Legionella rubrilucens* by visible light. *Eur. J. Microbiol. Immunol.* **7**, 146–149.
7. Dai, T., A. Gupta, Y.-Y. Huang, M. E. Sherwood, C. K. Murray, M. S. Vrahas, T. Kielian and M. R. Hamblin (2013) Blue light eliminates community-acquired methicillin-resistant *Staphylococcus aureus* in infected mouse skin abrasions. *Photomed. Laser Surg.* **31**, 531–538.
8. Maclean, M., S. J. MacGregor, J. G. Anderson and G. Woolsey (2009) Inactivation of bacterial pathogens following exposure to light

from a 405-nanometer light-emitting diode array. *Appl. Environ. Microbiol.* **75**, 1932–1937.
9. Makdoumi, K., M. Hedin and A. Bäckman (2019) Different photodynamic effects of blue light with and without riboflavin on methicillin-resistant *Staphylococcus aureus* (MRSA) and human keratinocytes in vitro. *Lasers Med. Sci*. [Epub ahead of print].
10. Ashkenazi, H., Z. Malik, Y. Harth and Y. Nitzan (2003) Eradication of *Propionibacterium acnes* by its endogenic porphyrins after illumination with high intensity blue light. *FEMS Immunol. Med. Microbiol.* **35**, 17–24.
11. Boyd, J. M., K. A. Lewis, N. Mohammed, P. Desai, M. Purdy, W.-H. Li, T. Fourre, D. Miksa, S. Crane, M. Southall and A. Fassih (2019) Propionibacterium acnes susceptibility to low-level 449 nm blue light photobiomodulation. *Lasers Surg. Med* **51**(8), 727–734.
12. Fan, X., Y.-Z. Xing, L.-H. Liu, C. Liu, D.-D. Wang, R.-Y. Yang and M. Lapidoth (2013) Effects of 420-nm intense pulsed light in an acne animal model. *J. Eur. Acad. Dermatol. Venereol.* **27**, 1168–1171.
13. Battisti, A., P. Morici, F. Ghetti and A. Sgarbossa (2017) Spectroscopic characterization and fluorescence imaging of Helicobacter pylori endogenous porphyrins. *Biophys. Chem.* **229**, 19–24.
14. Ganz, R. A., J. Viveiros, A. Ahmad, A. Ahmadi, A. Khalil, M. J. Tolkoff, N. S. Nishioka and M. R. Hamblin (2005) *Helicobacter pylori* in patients can be killed by visible light. *Lasers Surg. Med.* **36**, 260–265.
15. Lembo, A. J., R. A. Ganz, S. Sheth, D. Cave, C. Kelly, P. Levin, P. T. Kazlas, P. C. Baldwin, W. R. Lindmark, J. R. McGrath and M. R. Hamblin (2009) Treatment of Helicobacter pylori infection with intra-gastric violet light phototherapy: A pilot clinical trial. *Lasers Surg. Med.* **41**, 337–344.
16. Pummer, A., H. Knüttel, K.-A. Hiller, W. Buchalla, F. Cieplik and T. Maisch (2017) Antimicrobial efficacy of irradiation with visible light on oral bacteria in vitro: A systematic review. *Future Med. Chem.* **9**, 1557–1574.
17. Song, H.-H., J.-K. Lee, H.-S. Um, B.-S. Chang, S.-Y. Lee and M.-K. Lee (2013) Phototoxic effect of blue light on the planktonic and biofilm state of anaerobic periodontal pathogens. *J. Peridontal Implant Sci.* **43**, 72–78.
18. Maclean, M., S. J. Macgregor, J. G. Anderson, G. A. Woolsey, J. E. Coia, K. Hamilton, I. Taggart, S. B. Watson, B. Thakker and G. Gettinby (2010) Environmental decontamination of a hospital isolation room using high-intensity narrow-spectrum light. *J. Hosp. Infect.* **76**, 247–251.
19. Murrell, L. J., E. K. Hamilton, H. B. Johnson and M. Spencer (2019) Influence of a visible-light continuous environmental disinfection system on microbial contamination and surgical site infections in an orthopedic operating room. *Am. J. Infect. Control* **47**, 804–810.
20. Endarko, E., M. Maclean, I. V. Timoshkin, S. J. MacGregor and J. G. Anderson (2012) High-intensity 405 nm light inactivation of *Listeria monocytogenes*. *Photochem. Photobiol.* **88**, 1280–1286.
21. Masson-Meyers, D. S., V. V. Bumah, G. Biener, V. Raicu and C. S. Enwemeka (2015) The relative antimicrobial effect of blue 405 nm LED and blue 405 nm laser on methicillin-resistant *Staphylococcus aureus* in vitro. *Lasers Med. Sci.* **30**, 2265–2271.
22. Nitzan, Y. and M. Kauffman (1999) Endogenous porphyrin production in bacteria by δ-aminolaevulinic acid and subsequent bacterial photoeradication. *Lasers Med. Sci.* **14**, 269–277.
23. Fernandez, J. M., M. D. Bilgin and L. I. Grossweiner (1997) Singlet oxygen generation by photodynamic agents. *J. Photochem. Photobiol. B* **37**, 131–140.
24. Menon, I. A., M. A. Becker, S. D. Persad and H. F. Haberman (1990) Quantitation of hydrogen peroxide formed during UV-visible irradiation of protoporphyrin, coproporphyrin and uroporphyrin. *Clin. Chim. Acta* **186**, 375–381.
25. Feuerstein, O., I. Ginsburg, E. Dayan, D. Veler and E. I. Weiss (2005) Mechanism of visible light phototoxicity on *Porphyromonas gingivalis* and *Fusobacterium nucleatum*. *Photochem. Photobiol.* **81**, 1186–1189.
26. Maclean, M., S. J. Macgregor, J. G. Anderson and G. A. Woolsey (2008) The role of oxygen in the visible-light inactivation of *Staphylococcus aureus*. *J. Photochem. Photobiol. B* **92**, 180–184.
27. Murdoch, L. E., K. McKenzie, M. Maclean, S. J. Macgregor and J. G. Anderson (2013) Lethal effects of high-intensity violet 405-nm light on *Saccharomyces cerevisiae*, *Candida albicans*, and on dormant and germinating spores of *Aspergillus niger*. *Fungal Biol.* **117**, 519–527.
28. Maclean, M., S. J. MacGregor, J. G. Anderson and G. Woolsey (2008) High-intensity narrow-spectrum light inactivation and wavelength sensitivity of *Staphylococcus aureus*. *FEMS Microbiol. Lett.* **285**, 227–232.
29. Tomb, R. M., T. A. White, J. E. Coia, J. G. Anderson, S. J. MacGregor and M. Maclean (2018) Review of the comparative susceptibility of microbial species to photoinactivation using 380–480 nm violet-blue light. *Photochem. Photobiol.* **94**, 445–458.
30. Arakane, K., A. Ryu, C. Hayashi, T. Masunaga, K. Shinmoto, S. Mashiko, T. Nagano and M. Hirobe (1996) Singlet oxygen (1 delta g) generation from coproporphyrin in *Propionibacterium acnes* on irradiation. *Biochem. Biophys. Res. Commun.* **223**, 578–582.
31. Yoshida, A., H. Sasaki, T. Toyama, M. Araki, J. Fujioka, K. Tsukiyama, N. Hamada and F. Yoshino (2017) Antimicrobial effect of blue light using *Porphyromonas gingivalis* pigment. *Sci. Rep.* **7**, 5225.
32. Cieplik, F., A. Späth, C. Leibl, A. Gollmer, J. Regensburger, L. Tabenski, K.-A. Hiller, T. Maisch and G. Schmalz (2014) Blue light kills *Aggregatibacter actinomycetemcomitans* due to its endogenous photosensitizers. *Clin. Oral. Investig.* **18**, 1763–1769.
33. Lipovsky, A., Y. Nitzan, H. Friedmann and R. Lubart (2009) Sensitivity of *Staphylococcus aureus* strains to broadband visible light. *Photochem. Photobiol.* **85**, 255–260.
34. Lubart, R., A. Lipovski, Y. Nitzan and H. Friedmann (2011) A possible mechanisms for the bactericidal effect of visible light. *Laser Ther.* **20**, 17–22.
35. Ramakrishnan, P., M. Maclean, S. J. MacGregor, J. G. Anderson and M. H. Grant (2016) Cytotoxic responses to 405nm light exposure in mammalian and bacterial cells: Involvement of reactive oxygen species. *Toxicol. In Vitro* **33**, 54–62.
36. Amin, R. M., B. Bhayana, M. R. Hamblin and T. Dai (2016) Antimicrobial blue light inactivation of Pseudomonas aeruginosa by photo-excitation of endogenous porphyrins: In vitro and in vivo studies. *Lasers Surg. Med.* **48**, 562–568.
37. Battisti, A., P. Morici, G. Signore, F. Ghetti and A. Sgarbossa (2017) Compositional analysis of endogenous porphyrins from *Helicobacter pylori*. *Biophys. Chem.* **229**, 25–30.
38. Fyrestam, J., N. Bjurshammar, E. Paulsson, A. Johannsen and C. Östman (2015) Determination of porphyrins in oral bacteria by liquid chromatography electrospray ionization tandem mass spectrometry. *Anal. Bioanal. Chem.* **407**, 7013–7023.
39. Fyrestam, J., N. Bjurshammar, E. Paulsson, N. Mansouri, A. Johannsen and C. Östman (2017) Influence of culture conditions on porphyrin production in *Aggregatibacter actinomycetemcomitans* and *Porphyromonas gingivalis*. *Photodiagn. Photodyn. Ther.* **17**, 115–123.
40. Hamblin, M. R., J. Viveiros, C. Yang, A. Ahmadi, R. A. Ganz and M. J. Tolkoff (2005) *Helicobacter pylori* accumulates photoactive porphyrins and is killed by visible light. *Antimicrob. Agents Chemother.* **49**, 2822–2827.
41. Kjeldstad, B., A. Johnsson and S. Sandberg (1984) Influence of pH on porphyrin production in *Propionibacterium acnes*. *Arch. Dermatol. Res.* **276**, 396–400.
42. Plavskii, V. Y., A. V. Mikulich, A. I. Tretyakova, I. A. Leusenka, L. G. Plavskaya, O. A. Kazyuchits, I. I. Dobysh and T. P. Krasnenkova (2018) Porphyrins and flavins as endogenous acceptors of optical radiation of blue spectral region determining photoinactivation of microbial cells. *J. Photochem. Photobiol. B* **183**, 172–183.
43. Wang, Y., X. Wu, J. Chen, R. Amin, M. Lu, B. Bhayana, J. Zhao, C. K. Murray, M. R. Hamblin, D. C. Hooper and T. Dai (2016) Antimicrobial blue light inactivation of gram-negative pathogens in biofilms: in vitro and in vivo studies. *J. Infect. Dis.* **213**, 1380–1387.
44. Nitzan, Y., M. Salmon-Divon, E. Shporen and Z. Malik (2004) ALA induced photodynamic effects on gram positive and negative bacteria. *Photochem. Photobiol. Sci.* **3**, 430–435.
45. Hessling, M., B. Spellerberg and K. Hoenes (2017) Photoinactivation of bacteria by endogenous photosensitizers and exposure to visible light of different wavelengths – a review on existing data. *FEMS Microbiol. Lett.* **364**(2), 12 pp.
46. Kjeldstad, B. and A. Johnsson (1986) An action spectrum for blue and near ultraviolet in activation of *Propionibacterium acnes*; with emphasis on a possible porphyrin photosensitization. *Photochem. Photobiol.* **43**, 67–70.

47. Webb, R. B. and M. S. Brown (1976) Sensitivity of strains of *Escherichia coli* differing in repair capability to far UV, near UV and visible radiations. *Photochem. Photobiol.* **24**, 425–432.
48. Enwemeka, C. S., D. Williams, S. K. Enwemeka, S. Hollosi and D. Yens (2009) Blue 470-nm light kills methicillin-resistant *Staphylococcus aureus* (MRSA) in vitro. *Photomed. Laser Surg.* **27**, 221–226.
49. Guffey, J. S. and J. Wilborn (2006) In vitro bactericidal effects of 405-nm and 470-nm blue light. *Photomed. Laser Surg.* **24**, 684–688.
50. Khan, S., M. R. P, A. Rizvi, M. M. Alam, M. Rizvi and I. Naseem (2019) ROS mediated antibacterial activity of photoilluminated riboflavin: A photodynamic mechanism against nosocomial infections. *Toxicol. Rep.* **6**, 136–142.
51. Maisch, T., A. Eichner, A. Späth, A. Gollmer, B. König, J. Regensburger and W. Bäumler (2014) Fast and effective photodynamic inactivation of multiresistant bacteria by cationic riboflavin derivatives. *PLoS ONE* **9**, e111792.
52. Wong, T.-W., C.-W. Cheng, Z.-J. Hsieh and J.-Y. Liang (2017) Effects of blue or violet light on the inactivation of *Staphylococcus aureus* by riboflavin-5'-phosphate photolysis. *J. Photochem. Photobiol. B* **173**, 672–680.
53. García-Angulo, V. A. (2017) Overlapping riboflavin supply pathways in bacteria. *Crit. Rev. Microbiol.* **43**, 196–209.
54. Hönes, K., F. Stangl, M. Sift and M. Hessling (2015) Visible optical radiation generates bactericidal effect applicable for inactivation of health care associated germs demonstrated by inactivation of *E. coli* and *B. subtilis* using 405-nm and 460-nm light emitting diodes. In Novel Biophotonics Techniques and Applications III. (Edited by A. Amelink and I.A. Vitkin), 95400T. SPIE - International Society For Optics and Photonics, Proceedings of SPIE Volume 9540 at European Conferences on Biomedical Optics, Munich, Germany, 24 June – 25 June 2015.
55. Knak, A., J. Regensburger, T. Maisch and W. Bäumler (2014) Exposure of vitamins to UVB and UVA radiation generates singlet oxygen. *Photochem. Photobiol. Sci.* **13**, 820–829.
56. Kjeldstad, B. (1987) Different photoinactivation mechanisms in *Propionibacterium acnes* for near-ultraviolet and visible light. *Photochem. Photobiol.* **46**, 363–366.
57. Hoenes, K., M. Hess, P. Vatter, B. Spellerberg and M. Hessling (2018) 405 nm and 450 nm photoinactivation of *Saccharomyces cerevisiae*. *Eur. J. Microbiol. Immunol.* **8**, 142–148.
58. Wang, Y., R. Ferrer-Espada, Y. Baglo, Y. Gu and T. Dai (2019) Antimicrobial blue light inactivation of *Neisseria gonorrhoeae*: Roles of wavelength, endogenous photosensitizer, oxygen, and reactive oxygen species. *Lasers Surg. Med* **51**(9), 815–823.
59. Asaduzzaman, M., M. Ohya, M. Akter, T. Hayakawa, H. Kumura and J. Wakamatsu (2018) Searching for high ZnPP-forming bacteria for application to meat products. In Proceedings of the International Congress of Meat Science and Technology, (Edited by E. Puolanne), Melbourne, Australia, 12 August-17 August 2018. Available at: http://icomst-proceedings.helsinki.fi. Accessed on 28 August 2019.
60. Corbiere Morot-Bizot, S., S. Leroy and R. Talon (2007) Monitoring of staphylococcal starters in two French processing plants manufacturing dry fermented sausages. *J. Appl. Microbiol.* **102**, 238–244.
61. Löfblom, J., R. Rosenstein, M.-T. Nguyen, S. Ståhl and F. Götz (2017) *Staphylococcus carnosus*: From starter culture to protein engineering platform. *Appl. Microbiol. Biotechnol.* **101**, 8293–8307.
62. de Maere, H., S. Chollet, J. de Brabanter, C. Michiels, H. Paelinck and I. Fraeye (2018) Influence of meat source, pH and production time on zinc protoporphyrin IX formation as natural colouring agent in nitrite-free dry fermented sausages. *Meat Sci.* **135**, 46–53.
63. Zhang, Y., Y. Zhu, J. Chen, Y. Wang, M. E. Sherwood, C. K. Murray, M. S. Vrahas, D. C. Hooper, M. R. Hamblin and T. Dai (2016) Antimicrobial blue light inactivation of *Candida albicans*: In vitro and in vivo studies. *Virulence* **7**, 536–545.
64. McDonald, R. S., S. Gupta, M. Maclean, P. Ramakrishnan, J. G. Anderson, S. J. Macgregor, R. M. D. Meek and M. H. Grant (2013) 405 nm Light exposure of osteoblasts and inactivation of bacterial isolates from arthroplasty patients: Potential for new disinfection applications? *Eur. Cells Mater.* **25**, 204–214.
65. Frankenberg, L., M. Brugna and L. Hederstedt (2002) *Enterococcus faecalis* heme-dependent catalase. *J. Bacteriol.* **184**, 6351–6356.
66. Ramsey, M., A. Hartke and M. Huycke (2014) The physiology and metabolism of Enterococci. In *Enterococci: From Commensals to Leading Causes of Drug Resistant Infection* (Edited by M. S. Gilmore, D. B. Clewell, Y. Ike and N. Shankar). Massachusetts Eye and Ear Infirmary, Boston, MA.
67. Hope, C. K., K. Billingsley, E. de Josselin Jong and S. M. Higham (2016) A preliminary study of the effects of pH upon fluorescence in suspensions of Prevotella intermedia. *PLoS ONE* **11**, e0158835.